Thermochimica Acta, 197 (1992) 295–306
Elsevier Science Publishers B.V., Amsterdam

Thermal behavior of mechanically amorphized talc

Jiefan Liao and Mamoru Senna

Faculty of Science and Technology, Keio University, 3-14-1 Hiyoshi, Yokohama 223 (Japan)

(Received 24 July 1991)

Abstract

Changes in the structure of talc and processes in its dehydration and transformation into enstatite due to mechanical activation have been studied. The structure of talc became amorphous in the early stages of grinding. A decrease in the dehydration temperature and the appearance of an exothermic DTA peak took place following mechanical activation. The amount of heat evolved, estimated from the DTA peak area, increased with grinding time, but the temperature of the exothermic peak remained constant at 822°C. During mechanical activation, substantial dehydration took place, indicating a preferential destruction of the central layer of talc comprising $Mg(OH)_2$, leaving highly mobile O^{2-}. The formation of enstatite from mechanically amorphized talc is explained by postulating the recombination of O^{2-} ions with the partially broken SiO_4 tetrahedra as the rate-determining step.

INTRODUCTION

With its thermal endurance, lubricity and chemical stability, talc has been widely used as one of the most important magnesium silicates. After dehydration, it turns into enstatite and is used as a raw material for conventional as well as modern ceramics. The importance of talc has stimulated scientific and technical studies in various directions over the last fifty years [1–10].

The use of talc is almost always preceded by comminution processes to obtain fine particulate material. Fine grinding is not just a simple process of size reduction but is to be interpreted as a complex process including the simultaneous change in physical and chemical properties known as the mechanochemical process. Mechanical amorphization is a typical mechanochemical process. It also includes the rapidly growing field of mechanical alloying [11].

Mechanical activation of hydrated solids like talc shows several specific features related to the change in state of H_2O or OH during crystallo-

---

Correspondence to: M. Senna, Faculty of Science and Technology, Keio University, 3-14-1 Hiyoshi, Yokohama 223, Japan.

graphical degradation under mechanical stress [12,13]. Changes in the thermal behavior of some hydrated solids due to mechanical activation have been investigated [14,15]. But talc has not been sufficiently studied, in spite of its long history in silicate chemistry. The purpose of the present study is to obtain some fundamental insights into the effects of mechanical activation on the amorphization and thermal behavior of talc.

EXPERIMENTAL

Starting material and mechanical activation

Indian talc was crushed into particles smaller than 60 mesh sieve size (250 μm) for use as the starting material. According to the electron beam microanalysis, the starting material contained SiO_2 (61.78 wt.%), MgO (37.17 wt.%), Al_2O_3 (0.51 wt.%), and Fe_2O_3 (0.54 wt.%). Mechanical activation was carried out using a laboratory-sized vibration mill (Glen–Creston) equipped with a water-cooling system and a steel cylindrical vessel (50 cm^3) containing 100 steel balls 6 mm in diameter. Vibration amplitude and frequency were kept constant at 50 mm and 12 Hz, respectively. One gram of talc was ground batchwise with varying grinding times. The main impurity introduced during grinding was iron. After grinding for 2 h, the equivalent amount of Fe_2O_3 increased to 1.9 wt.%.

Characterization

Differential thermal analysis (DTA) and thermogravimetry (TG) were carried out simultaneously (Thermoflex, Rigaku) by raising the temperature linearly (10 K min^{-1}) in a stream of N_2 with a flow rate of 200 cm^3 min^{-1} and using α-Al_2O_3 as the reference. X-ray diffraction (XRD) patterns were recorded on the X-ray diffractometer (Rigaku, CN2013), using Cu Kα radiation, a Ni filter and a graphite monochromator. The infrared spectra were recorded by means of an FT–IR spectrometer (BIO-RAD, FTS-65) by the KBr disc method. $BaCO_3$ and CaF_2 were used as reference standards for DTA and XRD analyses, respectively. Granulometrical and morphological changes were monitored by a centrifugal sedimentation particle-size analyzer (Horiba, CAPA500), with a dispersing medium of 0.2 wt.% aqueous solution of sodium hexametaphosphate, and by scanning electron microscopy (JEOL, JSM 5200).

RESULTS AND DISCUSSION

Change in the granulometrical parameter and morphology

The median particle size d_{50}, measured by sedimentation analysis, decreased markedly in the first minutes of grinding, as shown in Fig. 1. A

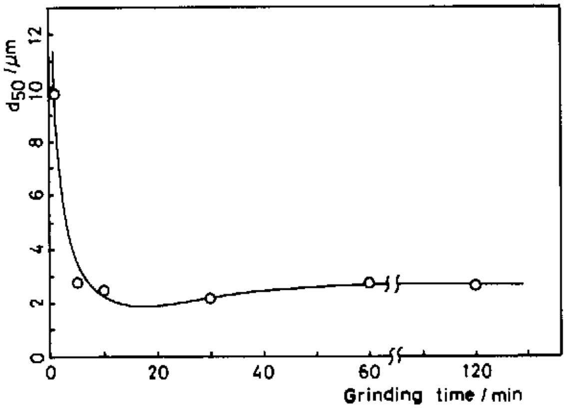

Fig. 1. Variation of the median particle size d_{50} with grinding time.

small increase in d_{50} after prolonged grinding is an indication of reagglomeration which is unavoidable in the finest grinding regime. The states of delamination at the beginning and agglomeration after prolonged grinding were observed under the scanning electron microscope, as shown in Fig. 2.

Weight loss during mechanical activation and heating

The weight loss of talc took place in two stages: the first stage from 495 to 605°C and the second from 845 to 1058°C for intact talc, as shown in Fig. 3, curve a. The profiles of thermogravimetry changed following mechanical activation as shown in Fig. 3, curves b to e. The bimodal weight loss curves suggest that there are two different routes of dehydration.

The composition of talc, often described as $Mg_3Si_4O_{10}(OH)_2$, can be alternatively expressed as $Mg_3Si_4O_{11-m}(OH)_{2m}$, with m being unity for the intact crystal. The weight loss during grinding was estimated from the total weight loss after thermogravimetry, because the decrease in the total thermal weight loss after grinding is to be interpreted as a result of partial dehydration during mechanical activation.

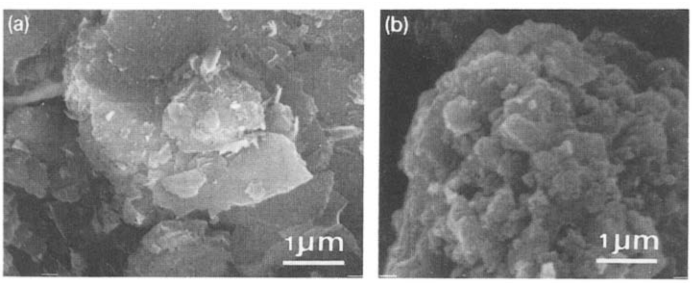

Fig. 2. Particle morphology of the samples after grinding for (a) 2 min and (b) 120 min.

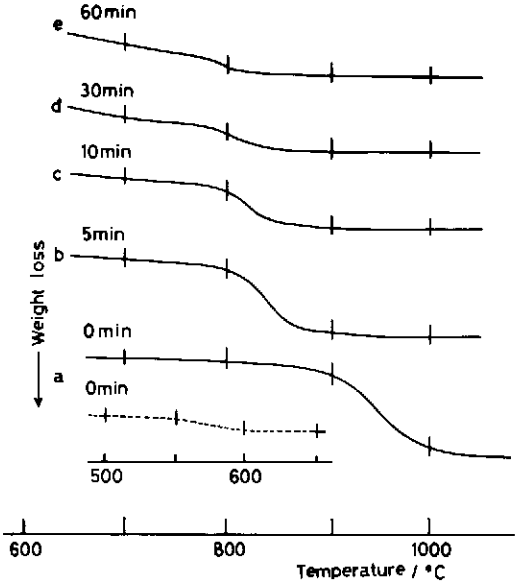

Fig. 3. Profiles of thermogravimetry for samples with different grinding times.

The values of m and T_{50}, the latter being the temperature at which 50% of the total weight loss took place on heating, decreased simultaneously with grinding time, as shown in Fig. 4.

A mechanically dehydrated species is not necessarily separated from the solid during grinding, but can remain on the surface of partially decomposed talc. Thus it seems reasonable to assume that the increase in the thermal weight loss at the first stage is attributed to the desorption of the adsorbed water molecules as a result of mechanical dehydration, whereas the weight loss at the second stage is due to loss of the hydroxyl groups still

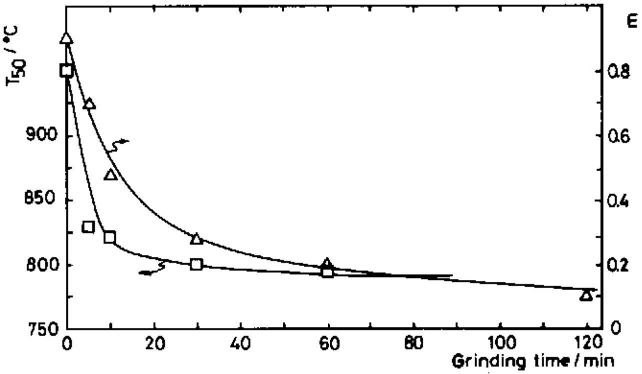

Fig. 4. Variation of temperature of 50% weight loss, T_{50}, and relative amount of water m with grinding time. Mechanically activated talc with partial dehydration is denoted as $Mg_3Si_4O_{11-m}(OH)_{2m}$ $(1 \geqslant m > 0)$, which defines m.

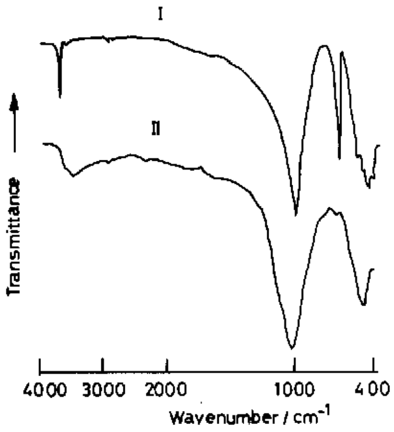

Fig. 5. IR spectra of the samples: curve I, initial talc; curve II, talc after grinding for 1 h.

bound to the bulk solid. The decrease in the dehydration temperature at the second stage therefore indicates the loosening of the bond between the hydroxyl group and the magnesium ion.

The change in the state of the OH group was therefore examined by IR spectroscopy. A fine sharp band at 3675 cm^{-1} observed on the initial talc, as shown in Fig. 5, curve I, is assigned to the OH stretching vibration in the octahedral layer of the talc structure, while those at 900–1100 cm^{-1} are due to the stretching vibration of Si–O bonds [16]. Another sharp absorption at 660 cm^{-1} on Fig. 5, curve I, belongs to the bending mode of H–O––Mg, and the complex absorption band in the region 450–490 cm^{-1} is due to the bending of Si–O.

After mechanical activation, the sharp band at 3675 cm^{-1} almost disappeared while a broad band in the region of 3500–3600 cm^{-1} appeared, as shown in Fig. 5, curve II. This new broad band may be attributed to the water molecules adsorbed on the surface of amorphized talc. These spectroscopic observations indicate that the state of –OH in talc changed after mechanical treatment. This is consistent with the observed partial dehydration and the decrease in T_{50} during grinding. It is also to be noted that the intensity and position of the bands due to the Si–O stretching and bending did not change significantly after grinding.

Change in the long-range ordering during mechanical activation

As shown in Fig. 6, the talc transformed into an amorphous structure during the early stages of grinding. The fractional amorphization D_a is defined as

$$D_a = 1 - \frac{I_t/I_s}{I_t^0/I_s^0} \qquad (1)$$

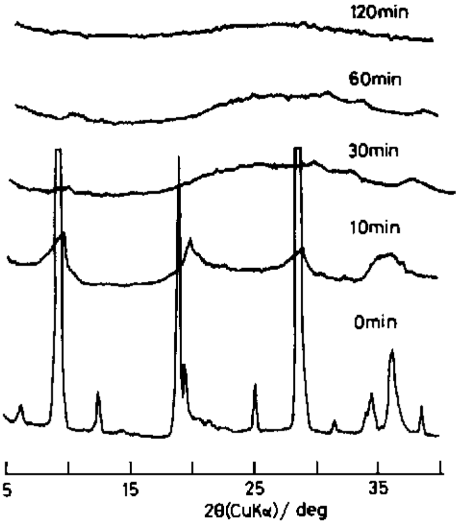

Fig. 6. XRD patterns of talc ground for varying grinding times.

where I_t is the intensity of the (002) diffraction peak of talc and I_s is the intensity of the (200) diffraction peak of the internal standard, CaF_2; I_t^0 and I_s^0 are, respectively, the values of I_t and I_s before grinding. D_a increased rapidly and reached almost unity after grinding for 60 min, as shown in Fig. 7. This indicates that the long-range ordering of talc was lost rapidly in the early stage of grinding.

Exothermic peak during heating amorphized talc

As shown in Fig. 8, no clear DTA peak was observed for the initial talc. Soon after grinding, however, an exothermic peak appeared at 822°C. It is to be noted that the position of the exothermic peak remained almost

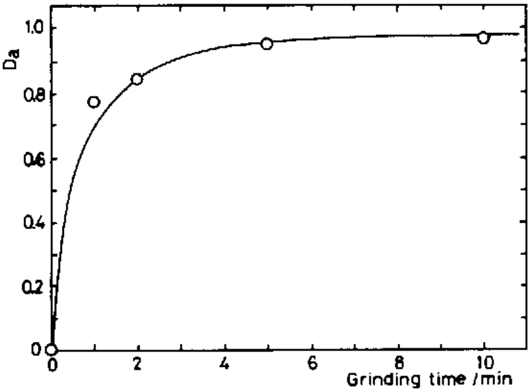

Fig. 7. Variation of fractional amorphization D_a with grinding time.

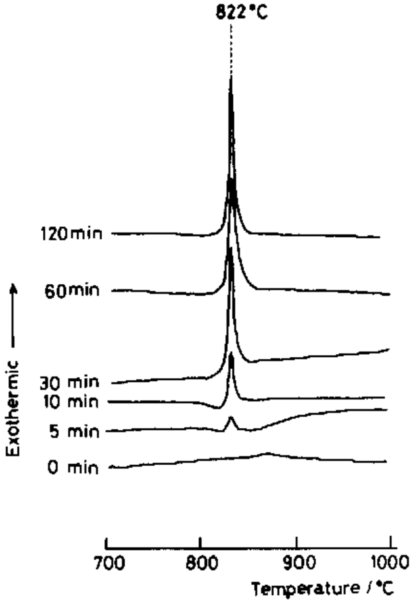

Fig. 8. DTA profiles of talcs with and without grinding.

unchanged, irrespective of the grinding time, while the peak intensity increased substantially with grinding. The amount of heat evolved, $-\Delta H$, increased with grinding time, as shown in Fig. 9. At the early stage of grinding, $-\Delta H$ increased markedly and then levelled off after 60 min. When $-\Delta H$ was plotted against D_a, no proportionality was found as also shown in Fig. 9. The observed change in the enthalpy cannot, therefore, be solely attributed to the heat of crystallization. It seems more appropriate to

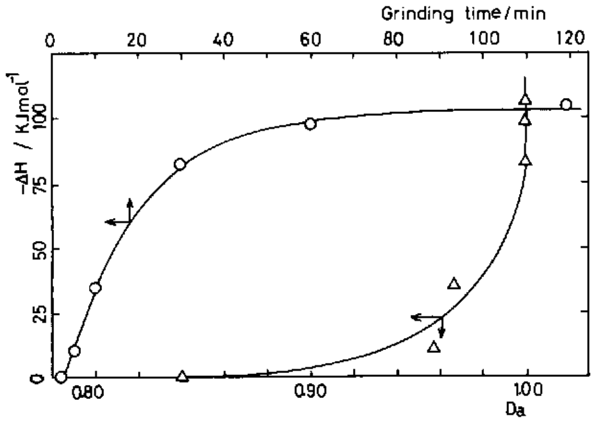

Fig. 9. Variation of the amount of heat evolved $-\Delta H$ with grinding time, and the relationship between $-\Delta H$ and D_a.

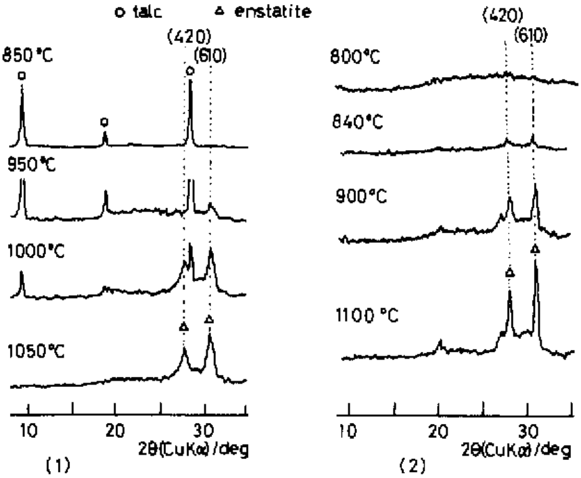

Fig. 10. XRD profiles of talcs after annealing at different temperatures: (1) initial talc and (2) talc after grinding for 1 h.

interpret the heat evolution as the result of the liberation of the energy stored during mechanical activation in the form of excess enthalpy [17].

The change in the XRD profile after annealing at different temperatures is shown in Fig. 10(1) and 10(2) for the initial and ground (60 min) talc, respectively. Enstatite was formed directly at about 950°C from the initial crystalline talc. In contrast, enstatite was formed from an amorphous state after T_p in the case of mechanically amorphized talc.

The crystallinity of the enstatite was higher, even after heating at temperatures well above the crystallization, e.g. at 1200°C, when talc was mechanically amorphized, as revealed from the increase in the intensity and the sharpness of the X-ray diffraction peak.

The IR spectra of the initial talc after heating at 850°C and 1050°C (the initial and final temperatures of dehydration, respectively) are shown in Fig. 11(1), curves I and II. For amorphized talc, the change in the spectra before and after T_p (800 and 840°C) is shown in Fig. 11(2). Heating up to the dehydration temperature for initial talc and T_p for amorphized talc brought about no significant changes in the spectrum.

Dehydration mechanism of crystalline talc

The mechanisms for the decomposition of talc that have been published are controversial [5–9]. It is at any rate necessary that the rearrangement of the SiO_4 tetrahedra changes from a two-dimensional layer in talc to a one-dimensional, parallel aligned chain in enstatite. From crystalline talc, the dehydration is immediately followed by the formation of enstatite. Hence, the change from talc to enstatite is topotactic [1]. One of the typical mechanisms which seems plausible is the so-called inhomogeneous mecha-

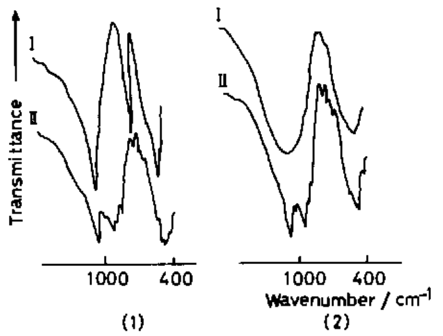

Fig. 11. IR spectra of the calcined talcs: (1) initial talc (curve I, heated at 850°C and curve II, 1050°C); (2) talc after grinding for 1 h (curve I, heated at 800°C and curve II, 840°C).

nism. According to the inhomogeneous mechanism proposed by Taylor [7], dehydration of talc occurs by a counter diffusion of Mg^{2+} and H^+ ions, whereas the oxygen packing in the acceptor regions is basically undisturbed. This is based on the hypothesis of simultaneous dehydration and enstatite formation: water molecules are formed in the donor region and subsequently removed, leaving pores and enstatite is formed in the acceptor region.

IR and XRD analyses in the present study indicate that the enstatite phase does not exist below T_p for mechanically amorphized talc, in spite of its large previous weight loss. Therefore the formation of enstatite from mechanically amorphized talc must have taken place via a mechanism different from that in the initial, well crystallized talc. Indeed, dehydration and crystallization of enstatite did not take place simultaneously for mechanically amorphized talc. In order to discuss further the behavior of the mechanically amorphized talc, it is necessary to consider the layer structure of talc.

Inhomogeneous destruction of the layer structure

Talc has a three-layered structure, i.e. two hexagonal silica layers sandwiching a central brucite layer [4]. This layer system is denoted as T–O–T. The chemical bonds involved in the structure of talc are divided into four types: ionic bonds between O and Mg; covalent bonds that are partly ionic between O and Si, and O and H; hydrogen bonds between O–H and O–Si, and van der Waals bonds between the T–O–T layer units. The van der Waals bonds are the weakest of all, leading to delamination at a very early stage of grinding, as shown in Fig. 2(a). Subsequent structural change on further grinding is mechanochemical dehydration. This can be expressed as

$$2(OH)^- \xrightarrow{\text{mechanical}} (1-m)H_2O + (1-m)O^{2-} + 2m(OH) \qquad (1 \geqslant m > 0) \qquad (2)$$

This should be the result of simultaneous breakage of the Mg–O and OH––(O–Si) bonds. At this stage, most of the energy supplied mechanically must have been used for mechanical activation, i.e. the reconstruction of the chemical bonds represented by eqn. (2), instead of size reduction. During mechanical activation of talc, $1-m$ oxygen ions are liberated as a result of mechanical dehydration as expressed by eqn. (2).

Energy storage in amorphized talc

The covalent bond between O and Si is the most difficult to break. This was shown by the change in the radial distribution function of mechanically amorphized silica [18]. As a result, the SiO_4 tetrahedra are very stable and the change in the connection angle takes place preferentially to the formation of dangling or broken bonds. Because the increase in the excess enthalpy was acute at the later stage of amorphization, as shown in Fig. 9, it is reasonable to assume that most of the excess energy is stored in the outer T layers in the form of apparently amorphous silica, rather than in the previously amorphized central layer. From the arguments given above, it is reasonable to conclude that the mechanical amorphization of talc does not take place uniformly throughout the T–O–T layer structure. Instead, the central part in the T–O–T structure of talc converts into the amorphous state preferentially, accompanied by the mechanochemical dehydration mentioned above. The later stage of the amorphization is associated with the plastic deformation of the outer silica layer, accompanied by the higher rate of energy storage.

Mechanism of enstatite formation from mechanically amorphized talc

When the mechanically activated talc is subjected to heating, magnesium metasilicate, amorphous silica and water molecules are produced

$$Mg_3Si_4O_{11-m}(OH)_{2m} \xrightarrow{\text{thermal}} 3MgSiO_3 + SiO_2 + mH_2O(1 \geqslant m > 0) \qquad (3)$$

The conversion of silicate minerals is always accompanied by a rearrangement of the linked SiO_4 tetrahedra. The reconstruction process involved during the reaction shown by eqn. (3) can be expressed as shown in Fig. 12, where the convention outlined in ref. 19 is adopted. It is necessary that free

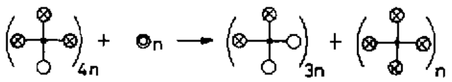

Fig. 12. Rearrangement of the linked SiO_4 tetrahedra during heating the mechanically activated talc: ●, silicon; ⊗, bridging oxygen, i.e. the oxygen shared with two tetrahedra; ○, non-bridging oxygen of SiO_4 tetrahedra; ⊙, free oxygen, i.e. the oxygen produced by mechanochemical dehydration. These notations are taken from ref. 19.

oxygen ions move to make the new ordering, a chain of tetrahedra being necessary to form enstatite. In other words, an increase in the amount of free O^{2-} ions during mechanical dehydration facilitates the formation of enstatite. On heating the mechanically activated talc, recombination of the free oxygen ions with the partly broken SiO_4 tetrahedra takes place, followed by their alignment to form parallel enstatite chains. The first step of the above-mentioned hypothetical process may be understood as a nucleation of enstatite from the apparently amorphized talc, and this may be the rate-determining process. In other words, it is postulated that the rate-determining process of enstatite formation from mechanically amorphized talc is the formation of a new order of Mg–O–Si with the highly mobile O^{2-} ions which have been produced by the preceding mechanochemical dehydration. The rate-determining process would therefore be independent of stored energy.

Once nuclei of enstatite are formed, the alignment of SiO_4 tetrahedra or the growth of the enstatite phase can easily take place, with the aid of the strain energy stored. The liberation of the stored energy at the alignment stage is thus visualized as the exothermic peak on the DTA profile, as shown in Fig. 8. This hypothetical mechanism also explains the insensitivity of the enstatite formation temperature to the grinding time, because the rate of nucleation is determined by the number of oxygen ions, which is independent of the stored energy.

Krönert et al. have published a study of the thermal behavior of "talc glass" which was also non-crystalline [9]. Unfortunately, however, there was no description of its preparation or of its thermal behavior. It is, therefore not possible to determine whether the behavior of the mechanically amorphized talc used in the present study has any similarity to that of talc glass.

CONCLUSION

Talc readily becomes amorphous under mechanical stress, but not as homogeneously as amorphous silica. The thermal properties change entirely following mechanical activation. An exothermic peak which appeared on the DTA profile of mechanically activated talc, did not change its position after further mechanical treatment. Formation of enstatite from mechanically amorphized talc took place via a mechanism different from that taking place from crystalline talc, due to the higher mobility of the O^{2-} ions formed as a result of preferential destruction and dehydration in the central brucite layer of the three-layered talc.

ACKNOWLEDGMENTS

We thank Dr. T. Isobe for valuable discussion and A. Sawabe for preliminary experimental work.

REFERENCES

1 J.F. Santos and K. Yada, Clays Clay Miner., 36 (1988) 289.

2 A.S. El-Hiti, Cent. Glass Ceram. Res. Inst. Bull., 30 (1983) 18.

3 R.H. Ewell, E.N. Bunting and R.F. Geller, J. Res. Natl. Bur. Stand., 15 (1935) 551.

4 J.D. Daw, P.S. Nicholson and J.D. Embury, J. Am. Ceram. Soc., 55 (1972) 149.

5 M. Koltermam, Neues Jahrb. Mineral. Monatsh., 41 (1964) 97.

6 S.B. Boskovic, M. Gasic, V.S. Nikolic and M.M. Ristic, Proc. Br. Ceram. Soc., 10 (1968) 1.

7 H.F.W. Taylor, Clay Miner. Bull., 5 (1962) 45.

8 W. Krönert, H.E. Schwiete and A. Suckow, Ziegelindustrie, 17 (1964) 337.

9 W. Krönert, H.E. Schwiete, and A. Suckow, Ziegelindustrie, 17 (1964) 364.

10 S.B. Boskovic, M. Gasic, B. Zivanovic and M.M. Ristic, Bull. Boris Kidric Inst. Nucl. Sci., 17 (1966) 115.

11 M.A. Hollanders, B.J. Thijsse and E.J. Mittemeijer, Colloq. Phys., 4 (1990) 101.

12 Y. Arai, T. Yasue and I. Yamaguchi, Nippon Kagaku Kaishi, (1972) 1395.

13 A. Ikekawa and S. Hayakawa, in G. Jimbo, M. Senna and Y. Kuwahara (Eds.), Proc. 2nd Japan–Soviet Symp. Mechanochemistry, Soc. Powd. Tech. Jpn. (Kyoto), p. 199.

14 Y. Arai and T. Yasue, Nippon Kagaku Kaishi, (1972) 198.

15 S. Inoue and M. Senna, React. Solids, 5 (1988) 155.

16 V. Stubican and R. Roy, J. Am. Ceram. Soc., 44 (1961) 625.

17 T. Isobe and M. Senna, J. Chem. Soc. Faraday Trans. 1, 84 (1988) 1199.

18 U. Steinike, U. Kertzschmar, I. Ebert and H.P. Hennig, React. Solids, 41 (1987) 1.

19 C.L. Babcock, Silicate Glass Technology Methods, Wiley, New York, 1977, p. 11.